engineering proceedings

MDPI

Proceeding Paper

Retention of Tuning for Vibro-Impact and Linear Dampers Under Periodic Excitation †

Petro Lizunov [1], Olga Pogorelova [2] and Tetyana Postnikova [2,*]

[1] Department of Structural Mechanics, Kyiv National University of Construction and Architecture, 31 Povitryanykh Syl Ave., 03680 Kyiv, Ukraine; lizunov@knuba.edu.ua
[2] Research Institute of Structural Mechanics, Kyiv National University of Construction and Architecture, 31 Povitryanykh Syl Ave., 03680 Kyiv, Ukraine; pogos13@ukr.net
* Correspondence: posttan@ukr.net
† Presented at the 6th International Electronic Conference on Applied Sciences, 9–11 December 2025; Available online: https://sciforum.net/event/ASEC2025.

Abstract

This work studies the ability of a single-sided vibro-impact nonlinear energy sink (SSVI NES) and a tuned mass damper (TMD) to maintain their vibration reduction performance when the natural frequency of the primary structure (PS), which is determined by its stiffness, changes. Both types of dampers demonstrate high efficiency in mitigating the PS vibrations under periodic excitation if their parameters are optimized at a specific PS natural frequency. Their ability to reduce PS vibrations changes similarly for both types of dampers when this structural parameter is changed.

Keywords: vibro-impact; damper; nonlinear energy sink; tuned mass damper; efficiency; tuning

1. Introduction

The problem of reducing unwanted vibrations in structures has been a concern of engineers and scholars for many years. Various solutions have been found, ranging from vibration isolation [1] to vibration control devices that are coupled to the main structure and can be active, passive, or hybrid. Passive control devices that do not require additional energy sources can be linear, such as tuned mass dampers (TMDs), and nonlinear, such as nonlinear energy sinks (NESs). TMDs have been widely discussed in the scientific literature and are still being discussed today. They have been implemented in engineering practice, particularly in several well-known structures. The papers [2,3] propose combining TMD with vibro-impact NES (VI NES). These comparative studies compare systems with TMD or VI NES and systems with TMD+VI NES. Optimal parameter values can optimize the performance of the coupled system. The systems are subjected to harmonic excitation, but in [2] the system is also subjected to seismic excitation. In the works [4,5], the authors examine the possibility of vibration control and vibration isolation using a mass-spring system with a semi-active damping coefficient focusing on application for reducing vehicle suspension vibration. NESs with cubic stiffness were proposed long ago, back in [6], but were widely discussed later, over the past two decades, within the framework of Targeted Energy Transfer (TET) theory. According to this theory, due to the system nonlinearity, NES takes part of the energy from the main structure and dissipates it. The shortcomings discovered in NESs encourage scientists to develop new types. The limitations of energy threshold and insufficient robustness in NESs are noted in [7]. The authors also point out insufficient adaptability of conventional NES in complex engineering environments.

Check for updates

Academic Editor: Ana Martins Amaro

Published: 3 February 2026

Copyright: © 2026 by the authors. Licensee MDPI, Basel, Switzerland. This article is an open access article distributed under the terms and conditions of the Creative Commons Attribution (CC BY) license.

Referring to [8], they note that conventional NESs possess certain limitations in practical applications. However, in their opinion, the damping performance and robustness of NESs can be significantly improved by introducing asymmetric stiffness characteristics. Parallel asymmetric NESs with three repulsive magnets are studied numerically and experimentally in [9]. Parameter optimization is performed using a genetic algorithm GA. Different types of NESs are discussed in [10,11]. In a recent article [11], the authors propose a novel device that combines a traditional tristable NES with cubic nonlinear damping. One study [12] investigates the efficiency of a double-sided vibro-impact nonlinear energy sink (VI NES) located in a cavity inside a linear oscillator. The efficiency is evaluated using the ratio of the energy dissipated by the VI NES to the total energy of the system. The authors optimize the parameters using deterministic (by a genetic algorithm GA) and stochastic optimization methods. A single-sided vibro-impact bistable NES designed for pulse and seismic control is examined in [13]. The asymmetric single-sided VI NES (SSVI NES) model is located on the top floor of the n-story construction to the right of an obstacle and has unlimited displacements in the direction opposite the obstacle. The authors note that the optimized parameters of this model are highly sensitive to the changes in initial velocity, while less sensitive to the stiffness of the PS.

This paper discusses the ability of SSVI NES and TMD to maintain their vibration reduction performance when the natural frequency of the primary structure changes. This phenomenon, when changing the damping of the primary structure and the external force intensity, was demonstrated in our previous paper [14]. The purpose of this work is to show that both SSVI NES and TMD demonstrate high efficiency in mitigating PS vibrations if their parameters are optimized at a certain value of the PS natural frequency. Their efficiency for both damper types changes in a similar way with changes in this structural parameter. This paper also aims to show how the tuning of the optimal SSVI NES and TMD design performed for a certain PS natural frequency is maintained or is not maintained when changing this natural frequency, as was shown in [14] for other structural parameters. The conclusions regarding the robustness of the tuning for these two damper types under periodic excitation can be considered as the novelty of this work.

2. Materials and Methods

A light damper (both SSVI NES and TMD) with mass m_2 is coupled to a heavy primary structure (PS) with mass m_1, which is a linear oscillator (Figure 1). The mass ratio $m_2/m_1 \cdot 100\% = 6\%$. Clearance C and initial distance D are optimized for SSVI NES, but selected with large values for TMD, which ensures the absence of impacts; i.e., the damper operates as linear.

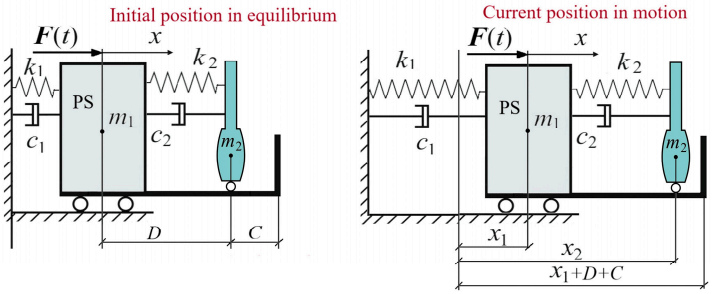


Figure 1. Conceptual scheme of a PS connected to a damper.

Harmonic exciting force $F(t) = Pcos(\omega t)$ acts on the PS. The repeated impacts on the obstacle and directly on the PS that occur during SSVI NES motion are simulated using a Hertz's nonlinear contact force according to his quasi-static contact theory [15]:

$F_{con}(z) = K \cdot \left[z(t)\right]^{\frac{3}{2}}$, where $z(t)$ is the rapprochement of the colliding bodies during an impact. Signorini's contact conditions are as follows:

$$\begin{array}{lll} x_1 \geq x_2, & z_1 = x_1 - x_2 & \text{for direct impacts on the PS,} \\ x_2 \geq x_1 + (D + C), & z_2 = x_2 - x_1 - (D + C) & \text{for impacts on an obstacle.} \end{array}$$

Coefficient K characterizes the mechanical and geometrical characteristics of colliding surfaces and varies for different surfaces:

$$K_i = \frac{4}{3} \frac{q_i}{(\delta_i + \delta_{i+1})\sqrt{A_i + B_i}}, \qquad \delta_i = \frac{1 - \nu_i^2}{\pi E_i}, \qquad i = 1,3.$$

Here, E_i and ν_i are the Young's moduli and Poisson's ratios of the four colliding surfaces; the constants A_i, B_i, and q_i are their joint geometrical characteristics, which are calculated according to the known table [15] depending on the type of contact surfaces. Assuming that both damper surfaces are spheres of large radii, and that PS and obstacle surfaces are flat, then $A_i = B_i = 1/2R_i$, where R_i is the large radius of the damper surfaces.

Combining Signorini's contact conditions and the Hertz contact law, and using the discontinuous Heaviside step function to "activate" the contact forces, we report the motion equations for this system in accordance with the fundamental law of dynamics as follows:

$$\begin{array}{l} m_1\ddot{x}_1 + c_1\dot{x}_1 + k_1x_1 - c_2(\dot{x}_2 - \dot{x}_1) - k_2(x_2 - x_1 - D) = F(t) - H(z_1)F_{con}(z_1) + H(z_2)F_{con}(z_2), \\ m_2\ddot{x}_2 + c_2(\dot{x}_2 - \dot{x}_1) + k_2(x_2 - x_1 - D) = H(z_1)F_{con}(z_1) - H(z_2)F_{con}(z_2). \end{array} \quad (1)$$

The initial conditions are as follows: $x_1(0) = 0$, $x_2(0) = D$, $\dot{x}_1(0) = \dot{x}_2(0) = 0$.

To solve the Cauchy problem, this stiff set of ordinary differential equations is integrated using the stiff solver *ode23s* from the *Matlab* platform(version R2011a), which provides a variable integration step and makes it extremely small at the impact points.

The dynamics of a system with a linear tuned mass damper is described by the same equations if there are no contact forces, which is determined by the zero values of the Heaviside function. Large values of the clearance C and initial distance D ensure its zero values and, consequently, the absence of contact forces.

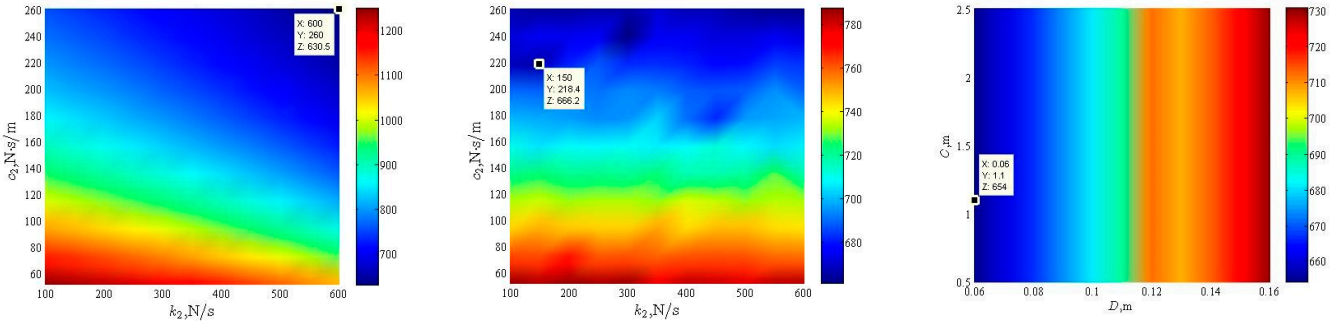
The dampers are designed to mitigate the PS vibrations, i.e., to reduce its mechanical energy, which is calculated by the well-known formula, where x_1(t) and $\dot{x}_1$(t) are the results of integration of the motion equations: $E_{1total}(t) = E_{1kinetic}(t) + E_{1poten}(t) = \frac{m_1\dot{x}_1(t)^2 + k_1x_1(t)^2}{2}$. The energy of the damper is $E_2(t) = \frac{m_2\dot{x}_2(t)^2 + k_2(x_2(t) - D)^2}{2}$.

The system parameters are as follows: m_1 = 1000 kg, m_2 = 60 kg, c_1 = 452 N·s/m, and P = 800 N. Mechanical characteristics of PS and obstacle surfaces are as follows: $E_1 = E_3 = 2.1 \cdot 10^{11}$ N/m^2, $\nu_1 = \nu_3 = 0.3$. Mechanical characteristics of damper surfaces are as follows: $E_2 = 2.21 \cdot 10^7$ N/m^2, $E_4 = 2.05 \cdot 10^7$ N/m^2, and $\nu_2 = \nu_4 = 0.4$. The PS natural frequency, determined by the PS stiffness, changes when the PS stiffness changes: $\omega_0 = \sqrt{k_1/m_1}$.

The optimal damper parameters are found using *Matlab* platform tools. The total mechanical energy of the $E_1(t)$ at each exciting force frequency is a function of time. Its maximum value E_{1max} is chosen as the objective function. The parameter optimization is carried out in two stages. In the first stage, the surface of the objective function is constructed using the *surf* program from the *Matlab* platform to select initial approximate parameter values (Figure 2).

In the second stage, the selected approximate parameter values taken from the Data Tip are refined using *fminsearch* program, which realizes local optimization using the Nelder–Mead method. A small change in the objective function values between iterations

can be considered as a convergence criterion; the optimization process can be believed as finalized (Table 1).



For TMD For SSVI NES For SSVI NES

Figure 2. Approximate optimal parameters of TMD and SSVI NES (m_2/m_1 = 6%, k_1 = 3.95·10^4 N/m).

Table 1. Fragment of *fminsearch* operation during optimization of SSVI NES parameters.

k_{2opt}, N/m	c_{2opt}, N·s/m	D_{opt}, m	C_{opt}, m	E_{1max}, J
1.500000E+002	2.184000E+002	6.000000E-002	1.100000E-001	6.662000E+002
2.100000E+002	2.184000E+002	6.000000E-002	1.100000E-001	6.611376E+002
2.203750E+002	2.334500E+002	6.037500E-002	3.622500E-001	5.731080E+002
⋮	⋮	⋮	⋮	⋮
2.150000E+002	2.320000E+002	6.000000E-002	3.600000E-001	5.630000E+002

The computational cost of optimization is moderate: each run of the algorithm requires several hundred calculations of the objective function, each of which is characterized by a low computational time.

3. Results and Discussion

The damper parameters after performing the optimization procedures are presented in Table 2.

Table 2. Optimized parameters of SSVI NES and TMD (m_2/m_1 = 6%, k_1 = 3.95·10^4 N/m).

Damper Type	m_2, kg	k_2, N/m	c_2, N·s/m	D, m	C, m
SSVI NES	60	215	232	0.06	0.36
TMD	60	600	262	2.08	4.7

The dampers with these optimized parameters ensure their high efficiency in mitigating the PS vibrations; i.e., they effectively reduce its maximum energy. However, having an optimal design found for PS stiffness k_1 = 3.95·10^4 N/m, they change their performance when PS stiffness changes. The maximum energy behavior for the PS without a damper and PS coupled to the SSVI NES and TMD with optimized parameters when changing the PS stiffness k_1 is shown in Figure 3.

In the version corresponding to the tuning shown in red, the best oscillation suppression is achieved. The SSVI NES provides two resonant peaks and reduces the PS vibrations in the resonance zone somewhat better than TMD. The mitigation is quite good for both the SSVI NES and the TMD at different PS stiffness values. Both damper types retain their tuning, but the TMD retains it somewhat better. With increasing PS stiffness k_1, the energy reduction remains virtually unchanged and remains identical for SSVI NES and TMD. When PS stiffness decreases, the energy reduction worsens; moreover, this deterioration

is greater for SSVI NES than for TMD. The resonance peak shifts to the left towards low frequencies. However, the energy reduction is maintained even at a significantly low stiffness value. The robustness of the damper tuning can be estimated using the ratio $Retention = E_{1max}(k_i)/E_{1max}(k_{opt})$. Based on this ratio, the tuning retention/degeneration rates over the tested k_1 variation range are presented in Table 3.

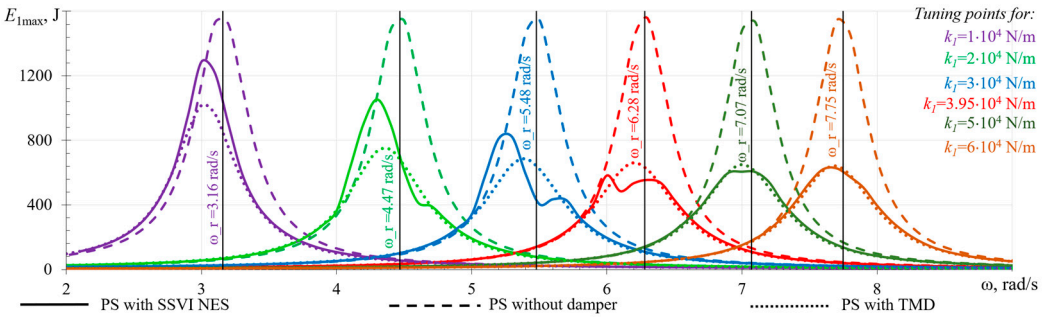


Figure 3. The reduction in maximum PS energy with attached SSVI NES and TMD tuned to k_1 = 3.95·10^4 N/m when changing the PS stiffness k_1.

Table 3. The robustness of damper tuning.

k_1, N/m	1·10^4	2·10^4	3·10^4	3.95·10^4	5·10^4	6·10^4
***Retention* SSVI NES**	2.21	1.81	1.41	1.00	1.04	1.08
***Retention* TMD**	1.54	1.12	1.03	1.00	0.981	0.970

The table clearly presents the results shown graphically in Figure 3. Specifically, the robustness of the damper tuning remains virtually unchanged with increasing PS natural frequency and deteriorates with its decrease. The deterioration of the TMD tuning is less than that of the SSVI NES. This fact can be explained as follows. First, the system with an attached TMD is linear and less sensitive to changes in the PS. Second, this model of SSVI NES with bilateral impacts, in which the direct impacts of SSVI NES on the PS occur, and which is essentially an asymmetric double-sided NES, is not the most successful model, as damper displacements in the direction opposite the obstacle are limited. The SSVI NES model with unlimited movements in the direction opposite to the obstacle [13] is more successful than the model with bilateral impacts. It is known that the advantages of NESs are most pronounced under transient loads, such as blast and seismic. Under periodic excitation, this model does not demonstrate the advantages of NESs.

Figure 4 demonstrates the areas of bilateral SSVI NES impacts on the PS directly and on the obstacle in pink, as well as areas of unilateral impacts only on the PS in blue, where there are no impacts on the obstacle. These graphs also show the E_{1max} curves for PS without dampers, with SSVI NES and TMD attached. The vertical black lines indicate the resonance frequency.

Bifurcation diagrams in Figure 4 demonstrate rich complex dynamics of the system with SSVI NES attached. The maximum energy of the PS with SSVI NES attached is shown as a dotted curve for clarity. The following notation is used here: nT, m, k regime is a mode with periodicity nT, where T is the period of the exciting force; m is the number of direct damper impacts on the PS per cycle; k is the number of damper impacts on the obstacle per cycle. The classification of response regimes is carried out by analyzing phase trajectories with Poincaré maps, Fourier spectra, and Lyapunov exponents, which allows us to distinguish between periodic and irregular modes, such as chaotic, intermittent, and transient chaos. For example, in last figure, the typical phase trajectories for three irregular regimes are shown. Amplitude-modulated regimes exhibit a typical specific form of the

time history of the displacements; the frequency of the envelope can be calculated using the Hilbert transform. In periodic regimes, the number of damper impacts per cycle directly on the PS m and on the obstacle k is calculated on the basis of graphs of contact forces and velocity jumps on phase trajectories, as well as graphs of the relationship of body displacements $(x_2 - x_1)$. The detailed description of rich complex dynamics of the system with SSVI NES attached should assist the design engineer, as irregular modes are difficult to control and the system behavior is difficult to predict.

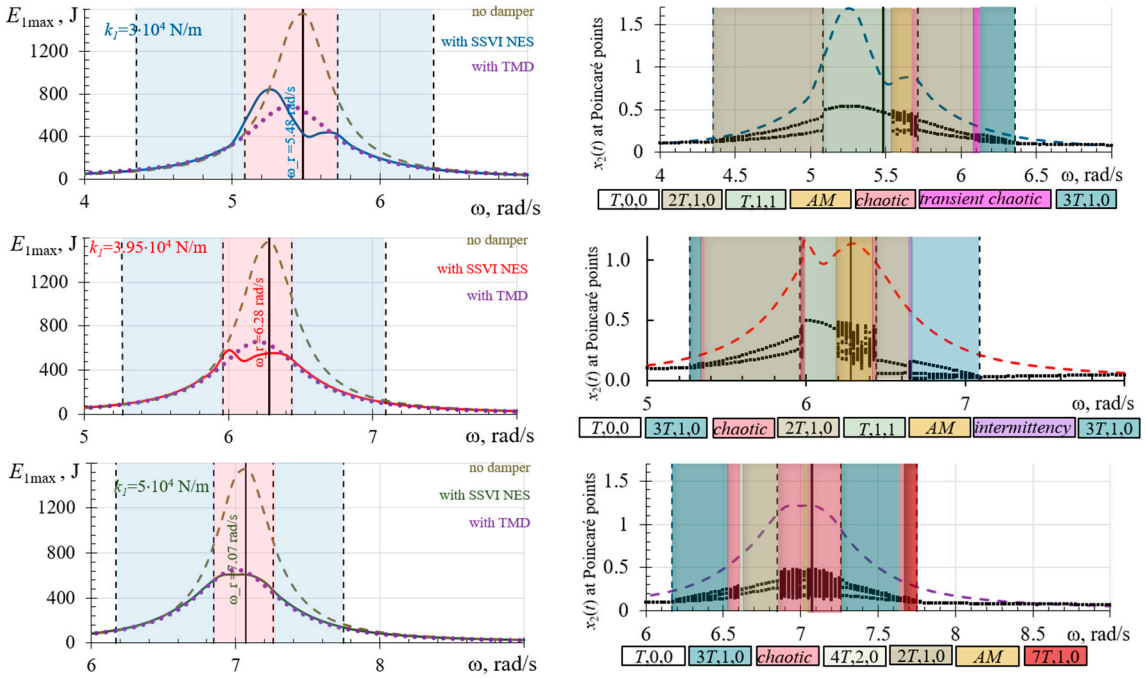


Figure 4. Graphs for three different values of PS stiffness k_1. (**Left**): The zones of SSVI NES bilateral impacts in pink and unilateral impacts on the PS only in blue. The maximum energy of PS without damper, with SSVI NES, and with TMD. (**Right**): Bifurcation diagrams of the system with SSVI NES.

The system dynamics differs for different k_1, but in all three graphs, the periodic regimes with different periodicity and different numbers of impacts alternate with various irregular regimes—chaotic, amplitude-modulated (AM), and intermittent. Some of them are shown below in last figure.

To clarify the energy transfer process between the PS and the damper, the energy ratios are calculated as follows: $R_1 = \frac{E_{1max}}{E_{1max}+E_{2max}}$ and $R_2 = \frac{E_{2max}}{E_{1max}+E_{2max}}$ [7]. These ratio values for different PS stiffness values k_1 are presented in Figure 5a. Figure 5b,c show the changes in these ratios as a function of the exciting force frequency ω for two k_1 values.

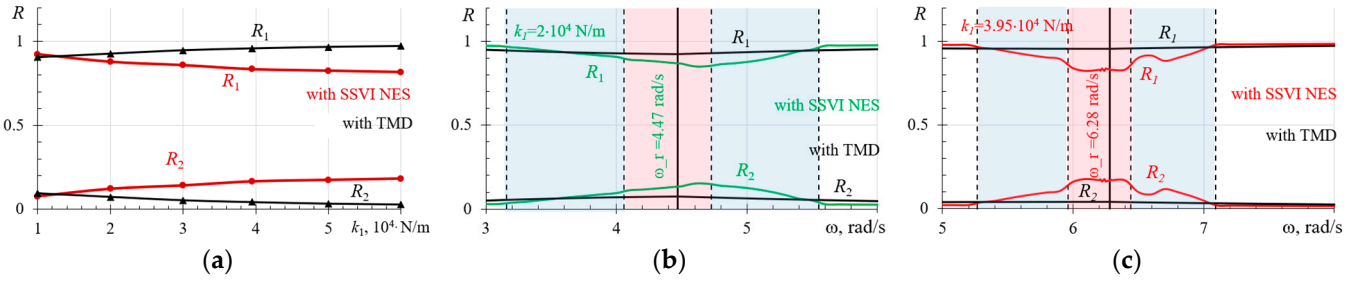
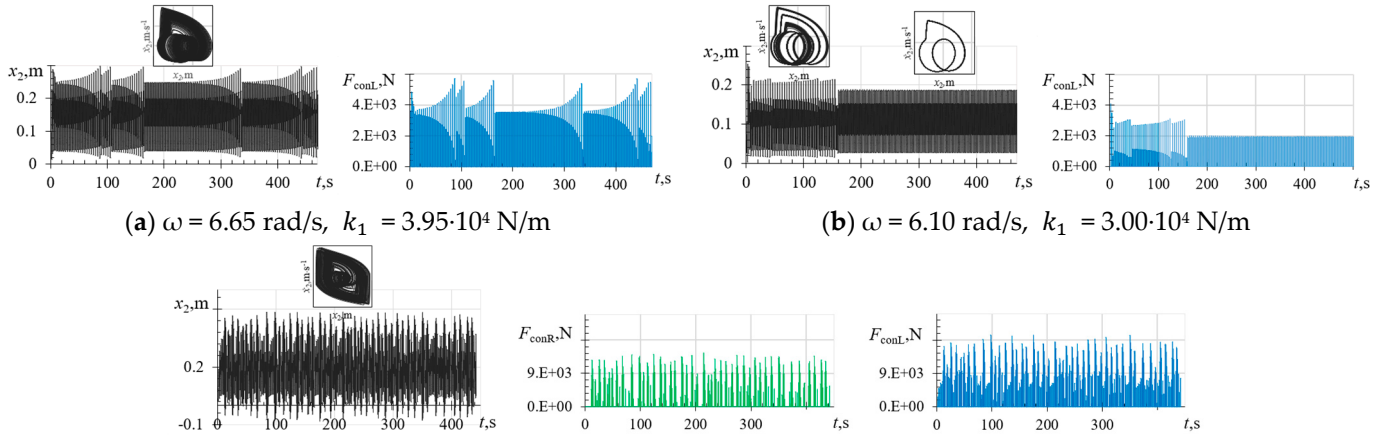


Figure 5. The energy ratios R_1 and R_2 (**a**) for different PS stiffness value k_1; (**b**) depending on exciting force ω for $k_1 = 2.00 \cdot 10^4$ N/m; (**c**) depending on exciting force ω for $k_1 = 3.95 \cdot 10^4$ N/m.

The richness of the complex dynamics of the system with the SSVI NES connected is characterized by various irregular modes. Some of these are shown in Figure 6. These graphs show the damper displacements $x_2(t)$, the phase trajectories characteristic for each movement, the contact forces during damper direct impacts on the PS F_{conL} in blue, and the contact forces during damper impacts on the obstacle F_{conR} in green at different exciting force frequencies ω, when the PS stiffness also varies.



(**a**) ω = 6.65 rad/s, k_1 = 3.95·10⁴ N/m (**b**) ω = 6.10 rad/s, k_1 = 3.00·10⁴ N/m

(**c**) ω = 7.10 rad/s, k_1 = 5.00·10⁴ N/m

Figure 6. (**a**) Intermittency with unilateral impacts. (**b**) Transient chaos with unilateral impacts. (**c**) Chaotic motion with bilateral impacts.

4. Conclusions

This study examined the ability of SSVI NES and TMD to maintain their reduction performance for PS under harmonic excitation when its stiffness changes. The study showed that both SSVI NES and TMD exhibit high efficiency in mitigating PS vibrations if their parameters are optimized at certain structural parameter values. They maintain their vibration reduction performance when the PS stiffness increases, but the PS energy reduction worsens when PS stiffness decreases. The deterioration in PS energy reduction is similar for both damper types, but the deterioration in reduction when using SSVI NES is slightly greater than when using TMD; i.e., TMD maintains its tuning a bit better. At the same time, SSVI NES is slightly better than TMD at transferring energy from the PS to the damper.

Author Contributions: Conceptualization, P.L. and O.P.; methodology, O.P.; software, T.P.; validation, P.L., O.P. and T.P.; formal analysis, O.P.; investigation, T.P.; writing—original draft preparation, T.P.; writing—review and editing, O.P.; visualization, T.P.; supervision, O.P.; project administration, P.L. All authors have read and agreed to the published version of the manuscript.

Funding: This research received no external funding.

Institutional Review Board Statement: Not applicable.

Informed Consent Statement: Not applicable.

Data Availability Statement: All the main data are contained in the article.

Conflicts of Interest: The authors declare no conflicts of interest.

References

1. Wu, S.; Yan, M.; Zhang, L.; Feng, L.; Yang, N. Nonlinear dynamic response of piecewise nonsmooth vibration isolation systems under base excitation. *J. Sound Vib.* **2026**, *624*, 119521. [CrossRef]

2. Di Egidio, A.; Briseghella, B.; Contento, A. Combined tuned mass damper and vibro-impacting nonlinear energy sink for the seismic protection of frame structures. *Structures* **2024**, *70*, 107576. [CrossRef]
3. Abdillahi, A.; Malekzadeh, M. Synergistic damping: Optimizing vibration control with TMDI and VI-NES integration in nonlinear systems. *SSRN* **2024**, *preprint*. [CrossRef]
4. Yang, Y.; Liu, C.; Chen, L.; Zhang, X. Phase deviation of semi-active suspension control and its compensation with inertial suspension. *Acta Mech. Sin.* **2024**, *40*, 523367. [CrossRef]
5. Yang, Y.; Liu, C.; Chen, L.; Zhang, X.; Zuo, L. Semi-active suspension with power-driven inerter and its performance evaluation. *J. Vib. Eng. Technol.* **2024**, *12*, 307–319. [CrossRef]
6. Roberson, R.E. Synthesis of a nonlinear dynamic vibration absorber. *J. Frankl. Inst.* **1952**, *254*, 205–220. [CrossRef]
7. Qi, X.; Zhang, J.; Wang, J. Dynamics and vibration reduction performance of an asymmetric nonlinear energy sink inspired by skeletal muscle mechanisms. *J. Sound Vib.* **2026**, *624*, 119523. [CrossRef]
8. Zeng, Y.; Ding, H.; Du, R.-H.; Chen, L.-Q. Micro-amplitude vibration suppression of a bistable nonlinear energy sink constructed by a buckling beam. *Nonlinear Dyn.* **2022**, *108*, 3185–3207. [CrossRef]
9. Guo, M.; Wu, Y.; Hu, C.; Tang, L.; Liu, K. Vibration suppression performance of tunable parallel asymmetric nonlinear energy sinks with distinct stability characteristics under impulse excitation. *J. Sound Vib.* **2025**, *624*, 119537. [CrossRef]
10. Fang, Y.; Ma, X.; Xia, X.; Yu, R.; Zhong, Y.; Zhang, Z. Dynamics-guided constrained optimization of a piezoelectric nonlinear energy sink for structural vibration control. *Eng. Struct.* **2026**, *346*, 121668. [CrossRef]
11. Li, X.; Qin, Y.; Lin, X.; Wang, Z.; Wang, L.; Yan, Z.; Nie, X. Parameter optimization and vibration control of tristable nonlinear energy sink incorporating with linear and nonlinear damping under impact excitation. *Int. J. Dyn. Control* **2025**, *13*, 12. [CrossRef]
12. Abdollahi, A.; Bab, S. Improving vibration suppression by applying stochastic optimization to a coil-contained vibro-impact nonlinear energy sink within a linear oscillator framework. *Appl. Math. Model.* **2026**, *151*, 116479. [CrossRef]
13. Li, J.; Sun, B.-X.; Yu, G.-L. Vibration mitigation for high-rise buildings by a single-sided vibro-impact bistable nonlinear energy sink. *Soil Dyn. Earthq. Eng.* **2026**, *203*, 110083. [CrossRef]
14. Lizunov, P.; Pogorelova, O.; Postnikova, T. Tuning of vibro-impact nonlinear energy sinks under changing structural parameters. Part 1. *Strength Mater. Theory Struct.* **2025**, *114*, 11–22. [CrossRef]
15. Goldsmith, W. *The Theory and Physical Behaviour of Colliding Solids*; Edward Arnold Publishers Ltd.: London, UK, 1960.

Disclaimer/Publisher's Note: The statements, opinions and data contained in all publications are solely those of the individual author(s) and contributor(s) and not of MDPI and/or the editor(s). MDPI and/or the editor(s) disclaim responsibility for any injury to people or property resulting from any ideas, methods, instructions or products referred to in the content.